



HAL
open science

Resonant inelastic X-ray scattering study of spin-wave excitations in the cuprate parent compound $\text{Ca}_2\text{CuO}_2\text{Cl}_2$

Blair W Lebert, Mark P. M. Dean, Alessandro Nicolaou, Jonathan Pellicciari, Marcus Dantz, Thorsten Schmitt, Runze Yu, Masaki Azuma, John-Paul Castellan, Hu Miao, et al.

► **To cite this version:**

Blair W Lebert, Mark P. M. Dean, Alessandro Nicolaou, Jonathan Pellicciari, Marcus Dantz, et al.. Resonant inelastic X-ray scattering study of spin-wave excitations in the cuprate parent compound $\text{Ca}_2\text{CuO}_2\text{Cl}_2$. 2016. hal-01388544v3

HAL Id: hal-01388544

<https://hal.science/hal-01388544v3>

Preprint submitted on 14 Nov 2016 (v3), last revised 6 Mar 2017 (v4)

HAL is a multi-disciplinary open access archive for the deposit and dissemination of scientific research documents, whether they are published or not. The documents may come from teaching and research institutions in France or abroad, or from public or private research centers.

L'archive ouverte pluridisciplinaire **HAL**, est destinée au dépôt et à la diffusion de documents scientifiques de niveau recherche, publiés ou non, émanant des établissements d'enseignement et de recherche français ou étrangers, des laboratoires publics ou privés.

Resonant inelastic X-ray scattering study of spin-wave excitations in the cuprate parent compound $\text{Ca}_2\text{CuO}_2\text{Cl}_2$

B. W. Lebert,^{1,2} M. P. M. Dean,³ A. Nicolaou,² J. Pelliciani,⁴ M. Dantz,⁴ T. Schmitt,⁴ R. Yu,⁵ M. Azuma,⁵ J-P. Castellan,^{6,7} H. Miao,³ A. Gauzzi,¹ B. Baptiste,¹ and M. d'Astuto^{1,*}

¹*Institut de Minéralogie, Physique des Matériaux et de Cosmochimie (IMPMC), UMR CNRS 7590, Université Pierre et Marie Curie - case 115, 4, place Jussieu, 75252 Paris cedex 05, France*

²*Synchrotron SOLEIL, L'Orme des Merisiers, Saint-Aubin, Boîte Postale 48, 91192 Gif-sur-Yvette Cedex, France*

³*Department of Condensed Matter Physics and Materials Science, Brookhaven National Laboratory, Upton, USA*

⁴*Swiss Light Source, Paul Scherrer Institut, CH-5232 Villigen PSI, Switzerland*

⁵*Materials and Structures Laboratory, Tokyo Institute of Technology, 4259 Nagatsuta, Midori, Yokohama 226-8503, Japan*

⁶*Laboratoire Léon Brillouin (CEA-CNRS), CEA-Saclay, F-91191 Gif-sur-Yvette, France*

⁷*Institute for Solid State Physics, Karlsruhe Institute of Technology, D-76021 Karlsruhe, Germany*
(Dated: November 14, 2016)

Resonant inelastic x-ray scattering was performed at the Cu L_3 edge on the undoped cuprate $\text{Ca}_2\text{CuO}_2\text{Cl}_2$. The spin wave dispersion along $\langle 100 \rangle$ and $\langle 110 \rangle$ was measured, yielding an estimate of the superexchange parameter $J = 160 \pm 10$ meV using a classical spin-1/2 2D Heisenberg model with nearest-neighbor interactions, or $J = 135 \pm 9$ meV including quantum fluctuations. The 45 meV dispersion along the zone boundary points $(0.5, 0)$ and $(0.25, 0.25)$ implies that next-nearest neighbor interactions in this compound are intermediate between the values in La_2CuO_4 and $\text{Sr}_2\text{CuO}_2\text{Cl}_2$. Comparison of our measurement of the spin superexchange parameter with quantum many-body calculations are easier, since $\text{Ca}_2\text{CuO}_2\text{Cl}_2$ is composed of only low Z atoms, and will help improve our understanding of the role of magnetic excitations and correlations in the cuprates.

PACS numbers: 74.72.Gh, 78.70.Ck

Keywords: Superconductivity, hole-doped cuprate, inelastic X-ray scattering

I. INTRODUCTION

Magnetic excitations have been studied intensely for their possible role in the Cooper pair formation which leads to high temperature superconductivity (HTS) in the cuprates.¹⁻⁴ These excitations have been studied in many of the cuprates using inelastic neutron scattering (INS)³. However, several pieces of the puzzle are still missing, largely due to the lack of a theoretical handling of correlated electronic systems beyond idealized, simplistic models.

Recently Cu L_3 edge resonant inelastic x-ray scattering (RIXS)^{5,6} has emerged as an alternative probe of the same excitations. The new technique extends INS observation to higher energies⁷, with the potential to also probe small volume crystals. However, it has mainly been used in the HTS cuprates to extend studies of compounds already measured by INS⁸. In that case, it is found that magnetic excitations persist up to very high dopings in regions of the Brillouin zone that are very difficult to measure using INS⁸.

The HTS cuprates $\text{Ca}_{2-x}\text{CuO}_2\text{Cl}_2$ and $\text{Ca}_{2-x}\text{Na}_x\text{CuO}_2\text{Cl}_2$ (Na-CCOC)⁹⁻¹¹ are vacancy and Na doped from the parent compound $\text{Ca}_2\text{CuO}_2\text{Cl}_2$ (CCOC). They are single layers with a simple quadratic structure, and without any structural phase transitions. Moreover, they are the only superconducting cuprates composed exclusively of low Z ions, with copper being the heaviest. This is an advantage for standard *ab-initio*

density functional theory calculations, where large Z ions pose problems for the pseudopotential optimization. It is even more advantageous for advanced methods trying to catch correlation effects, such as quantum Monte Carlo, where the strong spin-orbit coupling is highly challenging to treat accurately. Therefore in order to minimize relativistic effects, these quantum many-body calculations are mainly done on systems with light atoms, as pointed out by the authors of Ref. 12. $\text{Ca}_{2-x}\text{CuO}_2\text{Cl}_2$ and $\text{Ca}_{2-x}\text{Na}_x\text{CuO}_2\text{Cl}_2$ are the closest example to such systems among HTS cuprates. $\text{Ca}_{2-x}\text{Na}_x\text{CuO}_2\text{Cl}_2$ has been extensively studied by photoemission and scanning tunneling spectroscopy⁹⁻¹¹, therefore RIXS can help to provide a complete characterization of the system's quasiparticles. Here we study the parent compound of this HTS cuprate, $\text{Ca}_2\text{CuO}_2\text{Cl}_2$, and determine its spin-wave dispersion, from which we extract the superexchange parameter J using a simple numerical approximation based on the Heisenberg model Hamiltonian.

II. EXPERIMENTAL METHODS

A. Crystal growth and characterization

Single crystals of $\text{Ca}_2\text{CuO}_2\text{Cl}_2$ were grown from CaCO_3 , CuO , and CaCl_2 by solid state reaction^{13,14}. As shown in the top of Fig. 1, $\text{Ca}_2\text{CuO}_2\text{Cl}_2$ has a K_2NiF_4 -

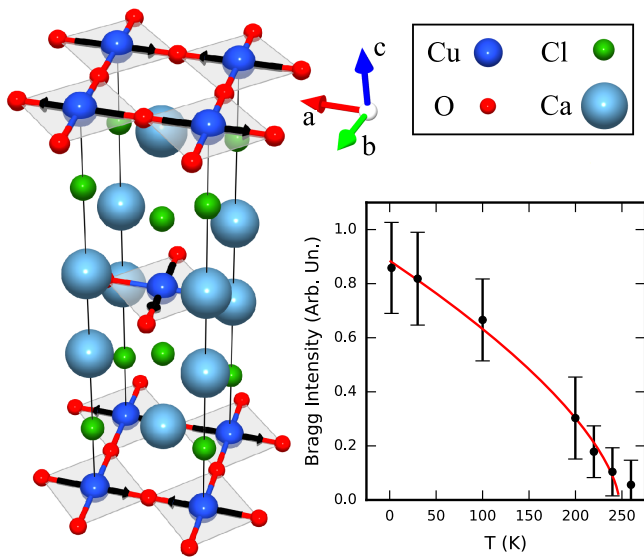


FIG. 1. (Color on line) (top left) Drawing¹⁷ of the $\text{Ca}_2\text{CuO}_2\text{Cl}_2$ unit cell¹⁴. The square coordination of copper with its four nearest-neighbor oxygen ions in the CuO_2 planes is shown. The chlorine ions are located in the apical site above and below the copper. Black arrows show one of the possible magnetic structures consistent with neutron diffraction¹⁶. (bottom right) Temperature dependence of the fitted intensity of the averaged Bragg reflections $(\frac{1}{2}, \frac{1}{2}, \frac{5}{2})$ and $(\frac{1}{2}, \frac{1}{2}, \frac{7}{2})$ and a power law fit (red).

type structure ($I4/mmm$)¹⁵ consisting of alternate stacking of the $(\text{Ca}, \text{Cl})_2$ layer and the single CuO_2 layer. The structure is similar to La_2CuO_4 with the apical oxygens replaced by chlorine and La replaced by Ca. The lattice parameters are $a=b=3.86735(2)$ and $c=15.0412(1)$ ^{13,14}. The crystals are easily cleaved along the ab -plane due to the weak ionic bonds within the $(\text{Ca}, \text{Cl})_2$ layer.

The single crystals (1-2 mm width/height and 0.2 mm thickness) were characterized using a Bruker 4-circle kappa geometry diffractometer. A fixed Mo anode was used and the filtered K_α emission was collimated at 0.2 mm (3 mrad). A cryogenic N_2 flux was used to isolate the sample from humidity since $\text{Ca}_2\text{CuO}_2\text{Cl}_2$ is highly hygroscopic. We found crystal parameters in agreement with literature^{13,14} and determined the crystal orientation with respect to visible facets. The samples were glued on the holder with silver epoxy and then ceramic posts were attached with the same epoxy.

$\text{Ca}_2\text{CuO}_2\text{Cl}_2$ is an antiferromagnetic insulator with a Néel temperature of $T_N = 247 \pm 5$ K¹⁶. To check the magnetic state of the samples we performed neutron scattering on the 1T spectrometer at Laboratoire Leon-Brillouin, using a sample from the same batch. We measured very weak magnetic reflections at low temperature for $\mathbf{q}=(\frac{1}{2}, \frac{1}{2}, \frac{\ell}{2})$ with $\ell=2n+1$ ($n=0, \dots, 4$), but none for $\ell=0$, in agreement with Ref. 16. The temperature dependence of the fitted Bragg intensity (average of the $(\frac{1}{2}, \frac{1}{2}, \frac{5}{2})$ and $(\frac{1}{2}, \frac{1}{2}, \frac{7}{2})$ reflections) is shown in the bottom

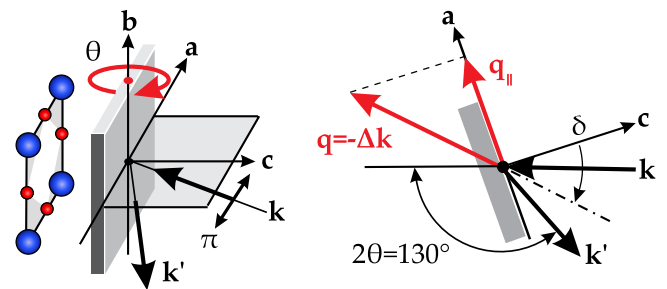


FIG. 2. (Color on line) RIXS geometry for measuring along $\langle 100 \rangle$ with π -polarization and grazing out emission (modified from Ref. 18). The scattering angle 2θ is defined between the incoming beam momentum \mathbf{k} and the direction where the analyzer collects the scattered beam \mathbf{k}' . 2θ and the azimuthal angles are fixed, whereas the incident angle can be changed by a rotation, θ , around the b -axis. The incident angle defines δ , which is the angle between the sample normal \mathbf{c} and the transferred momentum \mathbf{q} (red arrow), so that $\delta = 0$ in specular reflection. The projection of \mathbf{q} onto the sample's ab -plane is denoted \mathbf{q}_{\parallel} , which is 0 for $\delta = 0$ and maximal for grazing geometries. Measurements along $\langle 110 \rangle$ are done with the sample rotated 45° around the c -axis with respect to this figure.

right of Fig. 1 and a power law fit finds $T_N = 247 \pm 6$ K.

B. Resonant inelastic x-ray scattering

RIXS measurements at the Cu L_3 edge (930 eV) were performed at the ADDRESS beamline^{19,20} of the Swiss Light Source using the SAXES spectrometer²¹. The experiment geometry is shown in Fig. 2 and was similar to previous RIXS studies on cuprate parent compounds⁶. We used π -polarized incident x-rays and a grazing exit geometry in order to enhance the single magnon spectral weight^{7,22-27}.

The scattering angle was fixed at $2\theta = 130^\circ$, giving a constant momentum transfer to the sample of $q = 2k \sin(\theta) = 0.85 \text{ \AA}^{-1}$. Although q is fixed, its component in the ab -plane, q_{\parallel} , can be changed by rotating the sample about the vertical axis (b -axis in Fig. 2). For a given rotation, θ , the deviation from specular reflection is given as $\delta = \theta_{\text{specular}} - \theta$, thus $q_{\parallel} = q \sin(\delta)$. The minimum (maximum) δ used was $+5^\circ$ ($+55^\circ$) corresponding to $q_{\parallel} = +0.07 \text{ \AA}^{-1}$ ($q_{\parallel} = +0.70 \text{ \AA}^{-1}$). Therefore, in terms of reciprocal lattice units (r.l.u) in the ab -plane, we measured \mathbf{q}_{\parallel} from $(0.05, 0)$ to $(0.43, 0)$ along $\langle 100 \rangle$ and from $(0.03, 0.03)$ to $(0.3, 0.3)$ along $\langle 110 \rangle$. In other terms (Fig. 6 inset), we measured past the first Brillouin zone along Γ -M, but well short of where thermal neutrons measure at $M=(0.5, 0.5)$. Along Γ -X we measured very close to the first Brillouin zone edge at $X=(0.5, 0)$.

The samples were cleaved *in situ* using ceramic posts under ultra-high vacuum and low temperature conditions

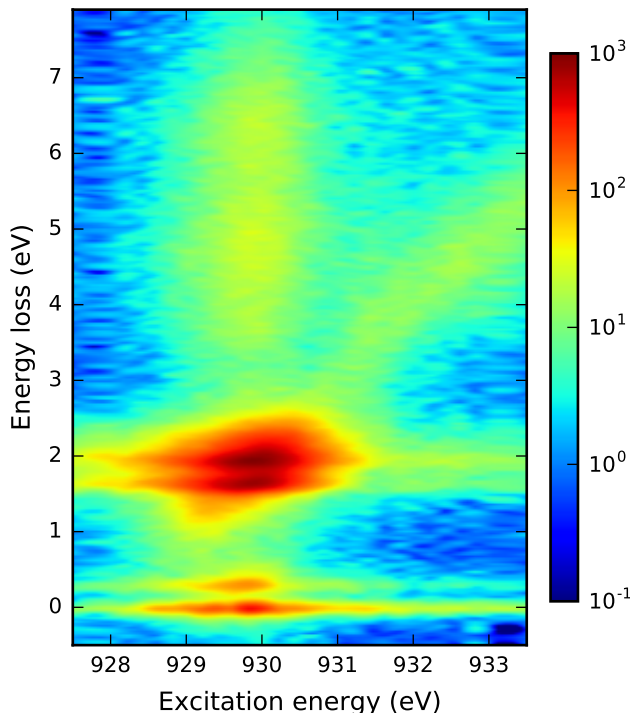


FIG. 3. (Color online) RIXS map at $\mathbf{q}_{\parallel} = (0.34, 0)$ with π incidence polarization showing the resonant behavior of the magnetic excitations, dd excitations, and charge transfer excitations. Weak fluorescence is seen at high energy when the system is excited above the Cu L_3 edge threshold. The colormap is a logarithmic scale in arbitrary intensity units.

to avoid hygroscopic damage. Their surface quality was confirmed with x-ray absorption spectroscopy. All spectra presented in this work were taken at 15 K.

III. RESULTS AND DISCUSSION

A RIXS map of $\text{Ca}_2\text{CuO}_2\text{Cl}_2$ at $\mathbf{q}_{\parallel} = (0.34, 0)$ is shown in Fig 3 and highlights the resonant behavior of the inelastic features. From lower to higher energy loss, there is a mid-infrared peak between 0.1 eV and 0.6 eV, dd excitations between 1 eV and 3 eV, and weak charge transfer excitations at higher energies. A weak fluorescence line is visible at energies above the Cu L_3 edge and intersects the dd excitations at resonance. The spectral weight from this fluorescence line at resonance is unknown, but it is likely appreciable as evidenced by the diagonal skew of the dd excitations.

In Fig. 4 the RIXS spectra obtained along both directions are shown in false color, while Fig. 5(a) shows line plots for $\delta = +10$ and $+55$. The spectra are normalized to the area of the dd excitations to account for the geometrical changes of the RIXS cross-section. There is an expected increase in elastic scattering near specular, i.e at $(0.09, 0)$ and $(0.06, 0.06)$. However, the elastic line for the sample aligned along $\langle 100 \rangle$ was large for all momen-

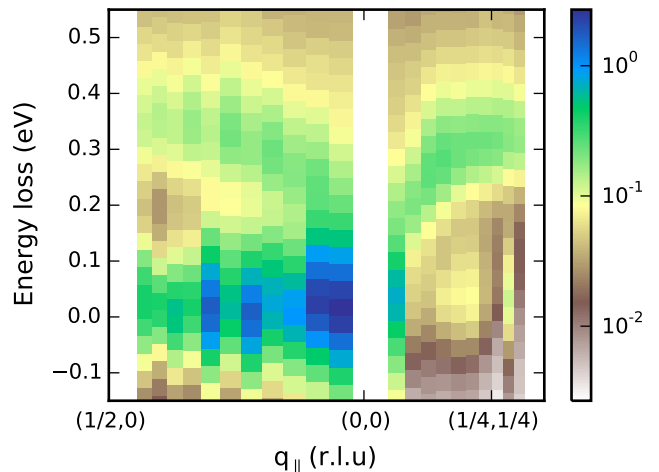


FIG. 4. (Color on line) False color plot of RIXS spectra along two high-symmetry directions. The colormap is a logarithmic scale of the intensity normalized by the area of the dd excitations.

tum transfers. These variations are likely due to finite surface quality after cleaving and did not impede accurate fitting of the magnetic features, which are clear in Fig. 4.

The mid-infrared feature is assigned as a magnon with a higher energy multi-magnon continuum. This assignment was done considering its dispersion (Fig. 4,6) and past RIXS results on cuprate parent compounds in this experiment geometry^{6,7}. Furthermore, in our case, magnetic excitations are the only excitation in the mid-infrared energy region due to the ≈ 2 eV Mott gap. These spin excitations are the focus of our paper and are discussed below.

The apical chlorine in $\text{Ca}_2\text{CuO}_2\text{Cl}_2$ increases the tetragonal distortion much like for $\text{Sr}_2\text{CuO}_2\text{Cl}_2$, therefore based on Ref. 18 we assigned the dd excitation at 1.70 eV to Cu- $3d_{xy}$, 1.99 eV to Cu- $3d_{xz/yz}$, and higher energies in the shoulder to Cu- $3d_{3z^2-r^2}$. The dd excitations were not well fit following the technique of Ref. 18, possibly because of the fluorescence emission also present in this energy region or electron-phonon coupling²⁸.

The broad charge transfer feature centered around 5.5 eV did not show dispersion or significant intensity variations, in agreement with Cu K edge RIXS²⁹. The author of Ref. 29 assigned this feature as transitions to an excited state composed of symmetric contributions of a central Cu- $3d_{x^2-y^2}$ orbital and the surrounding O- $2p_{\sigma}$ orbitals. Cu K edge RIXS also found a dispersive Mott excitation from 2.35 to 3.06 eV along Γ -X and from 2.34 eV to 4.14 eV along Γ -M. Therefore, the Mott excitation will fall under the dd excitations for the majority of our momentum transfers, however, the Mott excitation at ≈ 3.4 eV for $\mathbf{q}_{\parallel} = (0.3, 0.3)$ is not visible in our results (Fig. 5(a)).

A typical fit of the mid-infrared region is shown for $\mathbf{q}_{\parallel} = (0.21, 0.21)$ in Fig. 5(b) and the extracted magnon

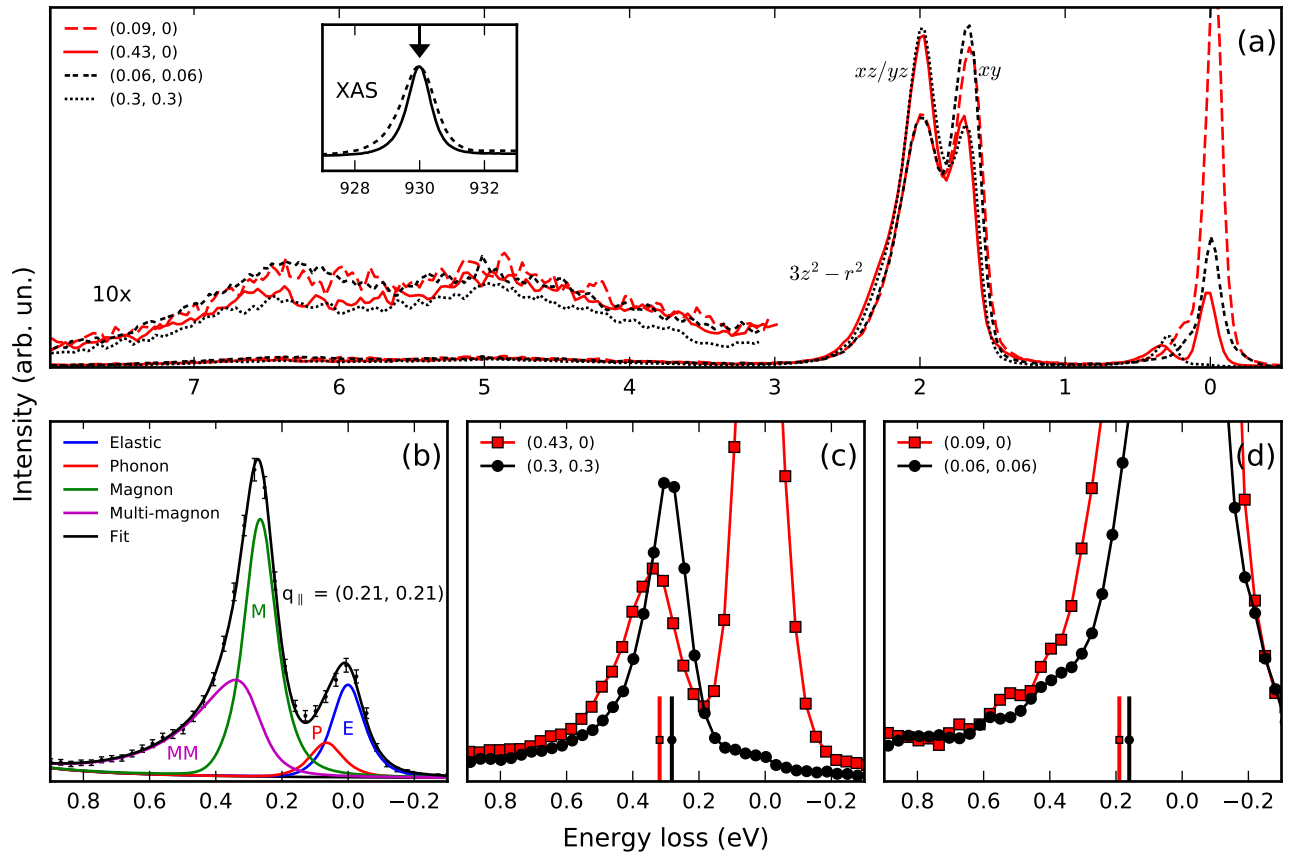


FIG. 5. (Color online) Cu L_3 RIXS spectra of $\text{Ca}_2\text{CuO}_2\text{Cl}_2$ at different in-plane transferred momentum, \mathbf{q}_{\parallel} , expressed as (h, k) in reciprocal lattice units. (a) Representative RIXS spectra along $\langle 100 \rangle$ (red) and $\langle 110 \rangle$ (black). All spectra have been normalized to the area of the dd excitations. The mid-infrared regions of these spectra are shown in (c,d), where vertical bars represent energy of single magnon found by fitting. The inset shows TEY-XAS (solid) and TFY-XAS (dashed), with an arrow indicating incident energy for our RIXS measurements. (b) Example of fitting procedure at $\mathbf{q}_{\parallel} = (0.21, 0.21)$ shown as black curve through data points. The elastic (E, blue), phonon (P, red), and single magnon (M, green) peaks were resolution-limited and the multi-magnon (M, magenta) peak fitting is described in the text.

dispersion is shown in Fig. 6. The elastic, phonon, and single magnon contributions were all resolution-limited. The elastic line was measured on carbon tape and showed a combined resolution of 130 meV full-width at half-maximum. The resolution function was well described using an arbitrary combination of two Gaussian functions and a Lorentzian function, which were multiplied by an intensity scaling factor during the fitting of all the spectra reported here. The multi-magnon excitation continuum was modeled as the resolution function convolved with a step function with subsequent exponential decay towards higher energy losses. The background was a Lorentzian tail of the form $y = A(x - x_0)^{-2} + c$. The energy of the phonon contribution is found around 60-70 meV with respect to the elastic, or ~ 15 -17 THz, roughly corresponding to the Debye cut-off frequency ω_D of $\text{Ca}_2\text{CuO}_2\text{Cl}_2$ ³⁰. The major source of uncertainty for the magnon energy was determining the elastic energy, since the elastic line was irregular for the sample aligned along $\langle 100 \rangle$ and often too weak along $\langle 110 \rangle$. Therefore, the elastic energy was fixed during fitting with respect to

the energy of the non-dispersive Cu- $3d_{xz/yz}$ orbital excitation, which was found to be 1.985 eV from several spectra with well-defined elastic lines.

The experimental and calculated dispersion along the two high-symmetry directions are shown together in Fig. 6. The calculated dispersion corresponds to a classical $S = 1/2$ 2D Heisenberg model with superexchange coupling \mathbf{J} between the the spins \mathbf{S} of the i and j nearest-neighbor (NN) :

$$\mathcal{H} = \mathbf{J} \sum_{\langle i,j \rangle} \mathbf{S}_i \cdot \mathbf{S}_j \quad (1)$$

where \mathbf{J} has only an *in-plane* component J . In this simple case, using classical linear spin-wave theory^{31,32}, the dispersion for an *in-plane* wave-vector $\mathbf{q}_{\parallel} = (h, k)$ is linear in J :

$$\hbar\omega_{\mathbf{q}} = 2J\sqrt{1 - [\cos(2\pi h) + \cos(2\pi k)]^2/4} \quad (2)$$

and the energy at the zone boundary peaks at $2J$, and we obtain $J = 160 \pm 10$ meV using the “SPIN-

WAVE” code³². Including spin quantum fluctuation renormalization^{33,34} we have:

$$\hbar\omega_{\mathbf{q}} = 2JZ_C\sqrt{1 - [\cos(2\pi h) + \cos(2\pi k)]^2/4} \quad (3)$$

where Z_C is a constant renormalization factor which lowers J to 135 ± 9 meV. This value is similar to other undoped cuprates such as La_2CuO_4 (136 ± 3 meV)³⁴ and $\text{Sr}_2\text{CuO}_2\text{Cl}_2$ (130 meV)⁷. Having a similar J reflects the fact that our data reaches a maximum energy at the zone boundary of 319 ± 10 meV, matching that of La_2CuO_4 (317 ± 7 meV) and slightly higher than $\text{Sr}_2\text{CuO}_2\text{Cl}_2$ (310 meV), although within experimental uncertainty.

There is a 45 ± 10 meV energy difference between the two BZ boundaries, (0.5,0) and (0.25,0.25), which cannot be explained with a simple NN Heisenberg model. This difference is an indication of extended magnetic interactions^{7,34} and was already observed in $\text{Sr}_2\text{CuO}_2\text{Cl}_2$ and La_2CuO_4 and . The behavior has been well described in terms of the Hubbard Hamiltonian in Ref. 7 and 35. Their results are interesting in terms of understanding the in-plane anisotropy of the spin dynamics, however it does not fundamentally change the estimation of the superexchange parameter from the NN model^{7,34}. The 45 meV energy difference between the two zone boundaries is larger than in La_2CuO_4 (22 ± 10 meV)³⁴ and smaller than in $\text{Sr}_2\text{CuO}_2\text{Cl}_2$ (70 meV)⁷, possibly indicating that $\text{Ca}_2\text{CuO}_2\text{Cl}_2$ has a larger (smaller) contribution from exchange terms beyond nearest-neighbors, with respect to La_2CuO_4 ($\text{Sr}_2\text{CuO}_2\text{Cl}_2$). Using additional exchange terms beyond NN in a Heisenberg model for 2D cuprates^{36,37} gives an energy of $\approx 2.2J$ at (0.5,0), corresponding to $J \approx 145$ meV for our results.

IV. CONCLUSIONS

We performed Cu L_3 edge RIXS on the undoped, antiferromagnetic HTS cuprate parent compound $\text{Ca}_2\text{CuO}_2\text{Cl}_2$. We measured the spin wave dispersion along the two high-symmetry directions and determined the leading exchange term $J = 160 \pm 10$ meV from a classical $S = 1/2$ 2D Heisenberg model with nearest-neighbor exchange. Including spin quantum fluctuation renormalization, this corresponds to $J = 135 \pm 9$ meV. To our knowledge, this is the first measurement of the spin-wave dispersion and their zone-boundary energy in $\text{Ca}_2\text{CuO}_2\text{Cl}_2$ since INS has not been performed, nor two-magnon Raman scattering measurements. Due to the possibility of quantum many-body simulation for the low Z cuprate $\text{Ca}_2\text{CuO}_2\text{Cl}_2$, our results combined with future calculations will offer a unique comparison between experiment and state-of-the-art theory of correlated systems, which is currently unavailable for other HTS cuprates.

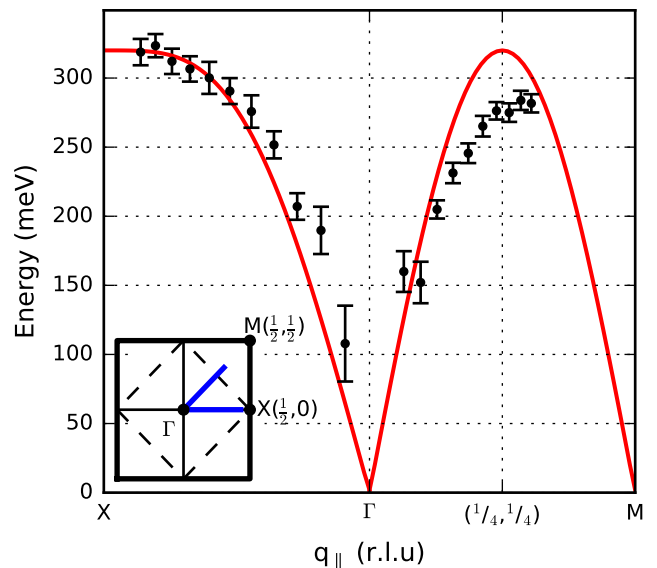


FIG. 6. (Color online) Dispersion of $\text{Ca}_2\text{CuO}_2\text{Cl}_2$ measured using Cu L_3 RIXS. The red line is a calculation for a classical spin-1/2 2D Heisenberg model with nearest-neighbor superexchange as described in the text. (inset) 2D Brillouin zone showing high-symmetry points. The first Brillouin zone boundary is represented by a dashed line, while the AFM zone boundary is represented by the thick black line. The region where we measured is shown as two thick blue lines along Γ -X and Γ -M.

ACKNOWLEDGMENTS

We acknowledge the Paul Scherrer Institut, Villigen-PSI, Switzerland for provision of synchrotron radiation beamtime at beamline X03MA, ”ADDRESS” of the Swiss Light Source, as well as LLB and KIT for providing neutron beamtime on 1T spectrometer, and would like to thank Yvan Sidis for his assistance. We are very grateful to Sylvain Petit for his help with ”SPINWAVE”. We thank Jean-Pascal Rueff and Marco Moretti for fruitful discussions. We thank Lise-Marie Chamoreau from the ”Plateforme Diffraction” at IPCM for help in sample diffraction. B.L acknowledges financial support from the French state funds managed by the ANR within the ”Investissements d’Avenir” programme under reference ANR-11-IDEX-0004-02, and more specifically within the framework of the Cluster of Excellence MATISSE led by Sorbonne Université and from the LLB/SOLEIL PhD fellowship program. This material is based upon work supported by the U.S. Department of Energy, Office of Basic Energy Sciences, Early Career Award Program under Award Number 1047478. J.P. and T.S. acknowledge financial support through the Dysenos AG by Kabelwerke Brugg AG Holding, Fachhochschule Nordwestschweiz, and the Paul Scherrer Institut. M.D. acknowledges financial support from the Swiss National Science Foundation within the D-A-CH programme (SNSF Research Grant 200021L 141325). M.d’A. acknowledges travel funding

from the E.C. under the 7th Framework Program within

the CALIPSO Transnational Access support.

- * matteo.dastuto@impmc.upmc.fr
- ¹ D. Scalapino, *Physics Reports* **250**, 329 (1995), ISSN 0370-1573, URL <http://www.sciencedirect.com/science/article/pii/037015739400086I>.
 - ² J. Orenstein and A. J. Millis, *Science* **288**, 468 (2000).
 - ³ Y. Sidis, S. Pailhès, B. Keimer, P. Bourges, C. Ulrich, and L. P. Regnault, *physica status solidi (b)* **241**, 1204 (2004), ISSN 1521-3951, URL <http://dx.doi.org/10.1002/pssb.200304498>.
 - ⁴ P. A. Lee, N. Nagaosa, and X.-G. Wen, *Rev. Mod. Phys.* **78**, 17 (2006), URL <http://link.aps.org/doi/10.1103/RevModPhys.78.17>.
 - ⁵ L. Braicovich, J. van den Brink, V. Bisogni, M. M. Sala, L. J. P. Ament, N. B. Brookes, G. M. De Luca, M. Salluzzo, T. Schmitt, V. N. Strocov, et al., *Phys. Rev. Lett.* **104**, 077002 (2010), URL <http://link.aps.org/doi/10.1103/PhysRevLett.104.077002>.
 - ⁶ M. Dean, *Journal of Magnetism and Magnetic Materials* **376**, 3 (2015), ISSN 0304-8853, pseudogap, Superconductivity and Magnetism, URL <http://www.sciencedirect.com/science/article/pii/S0304885314002868>.
 - ⁷ M. Guarise, B. Dalla Piazza, M. Moretti Sala, G. Ghiringhelli, L. Braicovich, H. Berger, J. N. Hancock, D. van der Marel, T. Schmitt, V. N. Strocov, et al., *Phys. Rev. Lett.* **105**, 157006 (2010), URL <http://link.aps.org/doi/10.1103/PhysRevLett.105.157006>.
 - ⁸ M. P. M. Dean, G. Dellea, R. S. Springell, F. Yakhov-Harris, K. Kummer, N. B. Brookes, X. Liu, Y.-J. Sun, J. Strle, T. Schmitt, et al., *Nat Mater* **12**, 1019 (2013), URL <http://dx.doi.org/10.1038/nmat3723>.
 - ⁹ Z. Hiroi, N. Kobayashi, and M. Takano, *Nature* **371**, 139 (2002).
 - ¹⁰ K. M. Shen, F. Ronning, D. H. Lu, F. Baumberger, N. J. C. Ingle, W. S. Lee, W. Meevasana, Y. Kohsaka, M. Azuma, M. Takano, et al., *Science* **307**, 901 (2005).
 - ¹¹ T. Hanaguri, C. Lupien, Y. Kohsaka, D.-H. Lee, M. Azuma, M. Takano, H. Takagi, and J. C. Davis, *Nature* **430**, 1001 (2004).
 - ¹² K. Foyevtsova, J. T. Krogel, J. Kim, P. R. C. Kent, E. Dagotto, and F. A. Reboredo, *Phys. Rev. X* **4**, 031003 (2014), URL <http://link.aps.org/doi/10.1103/PhysRevX.4.031003>.
 - ¹³ Y. Kohsaka, M. Azuma, I. Yamada, T. Sasagawa, T. Hanaguri, M. Takano, and H. Takagi, *Journal of the American Chemical Society* **124**, 12275 (2002), PMID: 12371870, <http://dx.doi.org/10.1021/ja026680i>, URL <http://dx.doi.org/10.1021/ja026680i>.
 - ¹⁴ I. Yamada, a. a. Belik, M. Azuma, S. Harjo, T. Kamiyama, Y. Shimakawa, and M. Takano, *Phys. Rev. B - Condens. Matter Mater. Phys.* **72**, 1 (2005), ISSN 10980121.
 - ¹⁵ H. Müller-Buschbaum, *Angewandte Chemie International Edition in English* **16**, 674 (1977), ISSN 1521-3773, URL <http://dx.doi.org/10.1002/anie.197706741>.
 - ¹⁶ D. Vaknin, L. L. Miller, and J. L. Zarestky, *Phys. Rev. B* **56**, 8351 (1997).
 - ¹⁷ K. Momma and F. Izumi, *J. Appl. Crystallogr.* **41**, 653 (2008).
 - ¹⁸ M. Moretti Sala, V. Bisogni, C. Aruta, G. Balestrino, H. Berger, N. B. Brookes, G. M. De Luca, D. Di Castro, M. Grioni, M. Guarise, et al., *New Journal of Physics* **13** (2011), ISSN 13672630, 1009.4882.
 - ¹⁹ V. N. Strocov, T. Schmitt, U. Flechsig, T. Schmidt, A. Imhof, Q. Chen, J. Raabe, R. Betemps, D. Zimoch, J. Krempasky, et al., *Journal of Synchrotron Radiation* **17**, 631 (2010), URL <http://dx.doi.org/10.1107/S0909049510019862>.
 - ²⁰ T. Schmitt, V. N. Strocov, K.-J. Zhou, J. Schlappa, C. Monney, U. Flechsig, and L. Patthey, *Journal of Electron Spectroscopy and Related Phenomena* **188**, 38 (2013), ISSN 0368-2048, progress in Resonant Inelastic X-Ray Scattering, URL <http://www.sciencedirect.com/science/article/pii/S0368204813000030>.
 - ²¹ G. Ghiringhelli, A. Piazzalunga, C. Dallera, G. Trezzi, L. Braicovich, T. Schmitt, V. N. Strocov, R. Betemps, L. Patthey, X. Wang, et al., *Review of Scientific Instruments* **77**, 113108 (2006), URL <http://scitation.aip.org/content/aip/journal/rsi/77/11/10.1063/1.2372731>.
 - ²² L. J. P. Ament, G. Ghiringhelli, M. M. Sala, L. Braicovich, and J. van den Brink, *Phys. Rev. Lett.* **103**, 117003 (2009), URL <http://link.aps.org/doi/10.1103/PhysRevLett.103.117003>.
 - ²³ M. W. Haverkort, *Phys. Rev. Lett.* **105**, 167404 (2010), URL <http://link.aps.org/doi/10.1103/PhysRevLett.105.167404>.
 - ²⁴ J.-i. Igarashi and T. Nagao, *Phys. Rev. B* **85**, 064422 (2012), URL <http://link.aps.org/doi/10.1103/PhysRevB.85.064422>.
 - ²⁵ M. Le Tacon, G. Ghiringhelli, J. Chaloupka, M. M. Sala, V. Hinkov, M. W. Haverkort, M. Minola, M. Bakr, K. J. Zhou, S. Blanco-Canosa, et al., *Nat Phys* **7**, 725 (2011), URL <http://dx.doi.org/10.1038/nphys2041>.
 - ²⁶ L. Braicovich, M. M. Sala, L. J. P. Ament, V. Bisogni, M. Minola, G. Balestrino, D. D. Castro, G. M. D. Luca, M. Salluzzo, G. Ghiringhelli, et al., *Phys. Rev. B* **81**, 174533 (2010).
 - ²⁷ M. P. M. Dean, A. J. A. James, R. S. Springell, X. Liu, C. Monney, K. J. Zhou, R. M. Konik, J. S. Wen, Z. J. Xu, G. D. Gu, et al., *Phys. Rev. Lett.* **110**, 147001 (2013), URL <http://link.aps.org/doi/10.1103/PhysRevLett.110.147001>.
 - ²⁸ J. J. Lee, B. Moritz, W. S. Lee, M. Yi, C. J. Jia, A. P. Sorini, K. Kudo, Y. Koike, K. J. Zhou, C. Monney, et al., *Phys. Rev. B* **89**, 041104 (2014), URL <http://link.aps.org/doi/10.1103/PhysRevB.89.041104>.
 - ²⁹ M. Z. Hasan, *Science (80-)*. **288**, 1811 (2000), ISSN 00368075, 0102489, URL <http://arxiv.org/abs/cond-mat/0102489http://www.sciencemag.org/cgi/doi/10.1126/science.288.5472.1811>.
 - ³⁰ M. d'Astuto, I. Yamada, P. Giura, L. Paulatto, A. Gauzzi, M. Hoesch, M. Krisch, M. Azuma, and M. Takano, *Phys. Rev. B* **88**, 014522 (2013), URL <http://link.aps.org/doi/10.1103/PhysRevB.88.014522>.
 - ³¹ A. Chubukov, E. Gagliano, and C. Balseiro, *Phys. Rev. B* **45**, 7889 (1992), URL <http://link.aps.org/doi/10.1103/PhysRevB.45.7889>.

- [1103/PhysRevB.45.7889](https://doi.org/10.1103/PhysRevB.45.7889).
- ³² S. Petit, in *JDN 18 - Neutrons et Simulations*, edited by N. M. M. Johnson and M. Plazanet (EDP Sciences, Les Ulis, 2011), vol. 12 of *JDN*, chap. Electronic Structure, Magnetism and Phonons, pp. 105 – 121.
- ³³ R. R. P. Singh, *Phys. Rev. B* **39**, 9760 (1989), URL <http://link.aps.org/doi/10.1103/PhysRevB.39.9760>.
- ³⁴ R. Coldea, S. M. Hayden, G. Aeppli, T. G. Perring, C. D. Frost, T. E. Mason, S.-W. Cheong, and Z. Fisk, *Phys. Rev. Lett.* **86**, 5377 (2001), URL <http://link.aps.org/doi/10.1103/PhysRevLett.86.5377>.
- ³⁵ B. Dalla Piazza, M. Mourigal, M. Guarise, H. Berger, T. Schmitt, K. J. Zhou, M. Grioni, and H. M. Rønnow, *Phys. Rev. B* **85**, 100508 (2012), URL <http://link.aps.org/doi/10.1103/PhysRevB.85.100508>.
- ³⁶ M. Dantz, J. Pelliciari, D. Samal, V. Bisogni, Y. Huang, P. Olalde-Velasco, V. N. Strocov, G. Koster, and T. Schmitt, *Scientific Reports* **6**, 32896 (2016), ISSN 2045-2322, arXiv:1608.05092v1, URL <http://www.nature.com/articles/srep32896>.
- ³⁷ N. S. Headings, S. M. Hayden, R. Coldea, and T. G. Perring, *Physical Review Letters* **105**, 247001 (2010), ISSN 0031-9007, URL <http://link.aps.org/doi/10.1103/PhysRevLett.105.247001>.